

ANRIL overexpression globally induces expression and alternative splicing of genes involved in inflammation in HUVECs

ALIMU WUFUER, XIEMUSIYE LUOHEMANJIANG, LEI DU, JING LEI,
MAYILA SHABIER, DENG FENG HAN and JIANHUA MA

Department of Neurology, The First Affiliated Hospital of Xinjiang Medical University, Urumqi, Xinjiang 830054, P.R. China

Received April 19, 2022; Accepted September 8, 2022

DOI: 10.3892/mmr.2022.12915

Abstract. Long non-coding (lnc)RNAs serve important cellular functions and certain lncRNAs have roles in different mechanisms of gene regulation. lncRNA-antisense non-coding RNA in the INK4 locus (ANRIL) affects cell inflammation; however, the potential genes underlying the inflammatory response regulated by ANRIL remain unclear. In the present study, the potential function of ANRIL in regulating gene expression and alternative splicing was assessed. ANRIL-regulated human umbilical vein endothelial cell (HUVEC) transcriptome was obtained using high-throughput RNA sequencing (RNA-seq) to evaluate the potential role of ANRIL. Following plasmid transfection, gene expression profile and alternative splicing pattern of HUVECs overexpressing ANRIL were analyzed using RNA-seq. ANRIL overexpression affected the transcription levels of genes associated with the inflammatory response, NF- κ B signaling pathway, type I interferon-mediated signal transduction pathway and innate immune response. ANRIL regulated the alternative splicing of hundreds of genes with functions such as gene expression, translation, DNA repair, RNA processing and participation in the NF- κ B signaling pathway. Many of these genes serve a key role in the inflammatory response. ANRIL-regulated inflammatory response may be achieved by regulating alternate splicing and transcription. The present study broadened the understanding of ANRIL-mediated gene regulation mechanisms and clarified the role of ANRIL in mediating inflammatory response mechanisms.

Introduction

Long non-coding (lnc)RNAs are defined as RNAs >200 nucleotides that are not translated into functional proteins. It is

well documented that a number of lncRNAs have important cellular functions and roles in different mechanisms of gene regulation. lncRNAs control the expression of nearby genes by influencing gene transcription. They can also interact with proteins by building complex secondary structures (1,2). lncRNAs can recruit chromatin remodeling complex and place them in nuclei at specific positions, thus regulating other chromosome-specific genes (3). The function of the encoded genes may involve structure and/or regulation, covering all stages of gene transcription and translation, including splicing, flipping and translation away from its genetic basis (4).

lncRNAs effect some physiological cell functions, while the changes in their expression are inherent in many diseases, such as ischemic stroke (IS) and cancer. In patients with ischemic injury or ischemic injury animal models, abnormal expression of lncRNAs have been reported using techniques such as microarray or RNA-sequencing (RNA-seq) (5). Specifically, uncoded antonym RNA has been identified in lncRNA gene bank entries for inhibitors of CDK4 (INK4), antisense non-coding RNA in the INK4 locus (ANRIL), H19, metastasis-associated lung adenocarcinoma transcript 1 (MALAT1), maternally expressed gene 3 and N1LR, which affect cell inflammation, apoptosis, angiogenesis and other physiological and pathological processes (6). ANRIL is present in more than eight splice variants that are ~3.9 kb in length (7), located on chromosome 9p21, which is association with myocardial infarction and IS (8). The regulation of gene expression by ANRIL is mediated by combining multiple fusion inhibitors of compound 1 or 2 (Polycomb repressive complex) and gene silencing is directed to the position INK4b-ARF-INK4a. Together, these findings indicate that ANRIL has a direct effect on the pathobiology of atherosclerosis. Therefore, ANRIL is considered a good candidate for atherosclerotic disease risk, such as coronary artery disease (CAD) and IS (9,10).

Inflammatory responses are involved in endothelial dysfunction, propagation of atherosclerosis and ischemic brain injury (11,12). Cerebral ischemia and ischemia-reperfusion injury cause an inflammatory cascade reaction, including inflammatory cell infiltration, release of toxic inflammatory mediators and oxidative stress and excitotoxicity, thus leading to further nerve tissue damage and cell death (13). Over recent years, multiple studies have reported that ANRIL regulates the inflammatory response and proliferation of cells through different signaling pathways in pathological aspects of ischemic

Correspondence to: Dr Jianhua Ma, Department of Neurology, The First Affiliated Hospital of Xinjiang Medical University, 137 Liyushan South Road, Urumqi, Xinjiang 830054, P.R. China
E-mail: 840296810@qq.com

Key words: antisense non-coding RNA in the INK4 locus, inflammatory response, RNA-seq, gene expression, alternative splicing

stroke (14-16). For example, Zhao reported that lncRNA ANRIL knockdown improves cerebral infarction-induced neurological deficits and decreases the number of apoptotic neurons in an animal model. The possible underlying mechanism may be related to the effect of inhibition of lncRNA ANRIL knockdown on the NF- κ B signaling pathway (17). Previous studies have also reported that in animal models of diabetes with cerebral ischemia, the increase of vascular endothelial growth factor (VEGF) is caused by overexpression of ANRIL and angiogenesis is achieved by activating the NF- κ B signaling pathway (17,18). However, it is unclear how ANRIL affects the expression of potential downstream genes that regulate endothelial dysfunction and inflammatory response.

To study the potential function of ANRIL in regulating expression and alternative splicing, ANRIL-regulated transcriptomes were assessed in human umbilical vein endothelial cells (HUVECs) using RNA-seq. The present study provided an important database and platform to evaluate the role of ANRIL in mediating the mechanisms of inflammatory response.

Materials and methods

Cell culture. HUVECs (cat. no. 8000; ScienCell Research Laboratories, Inc.) were cultured in extracellular matrix (ECM, 1001, ScienCell) at 37°C (with 5% CO₂ Atmosphere) containing 5% fetal bovine serum (1001, ScienCell) supplemented with 100 U/ml penicillin, 100 g/ml streptomycin and 1% growth factor (1001, ScienCell). The cultured cells were processed according to the manufacturer's protocols as follows: Original culture solution was aspirated, cells were washed using PBS, 0.05% trypsin (183, ScienCell) was used for digestion (37°C) for 2 min and Complete medium containing 10% fetal bovine serum was added to stop digestion. Cultured wells were blown into single cells using a pipette gun and a 15 μ l aliquot of cell suspension was counted, the remaining cell suspension was centrifuged at 143 x g for 5 min (37°C), resuspended with culture medium and were seeded (1x10⁵/well) into 24-well plates. Each group had 3 replicates and was cultured overnight at 37°C under 5% CO₂.

Plasmid transfection. After cells were plated and cultured overnight at 37°C, plasmid transfection was performed. HUVEC cells was performed using Lipofectamine 2000 (11668019, Invitrogen; Thermo Fisher Scientific, Inc.) according to the manufacturer's protocol. The ANRIL gene was constructed into pcDNA3.1 vector synthesized from Youbio Biotech and transfected to HUVEC cells with 500 ng plasmid. After incubated at 37°C for 24 h, they were used for RT-qPCR analysis. Following transfection, medium was replaced with fresh complete medium and incubated under 5% CO₂ at 37°C for 24 h and imaging was performed using a Optical light microscope. Samples were collected for subsequent experiments

Assessment of gene overexpression. GAPDH was used as an internal control gene to evaluate overexpression of ANRIL. Complementary DNA (cDNA) was synthesized as follows: The collected HUVEC cells were subjected to total RNA extraction using TRIZOL (15596-018, Ambion). The RNA was further purified with two phenol-chloroform treatments

and then treated with RQ1 DNase (M6101, Promega) to remove DNA. The quality and quantity of the purified RNA were determined by measuring the absorbance at 260/280 nm (A260/A280) using Smartspec Plus (Bio-Rad). The integrity of RNA was further verified by 1.5% agarose gel electrophoresis. Reverse transcription at 37°C for 15 min. Then for pre degeneration at 95°C for 10 min, 40 cycles of degeneration at 95°C for 15 sec, annealing and extension at 60°C for 1 min. Bio-Rad S1000 thermocycler was used for reverse transcription (RT)-PCR using SYBR-Green Bestar RT-PCR Master Mix (DBI Bioscience). The concentration of each transcript was standardized to the GAPDH mRNA expression level using the 2^{- $\Delta\Delta$ C_q} method (19). The thermocycling conditions were as follows: Denaturing at 95°C for 10 min, followed by 40 cycles of denaturing at 95°C for 15 sec and annealing and extension at 60°C for 1 min. PCR amplification was performed in triplicate for each sample. Primers for quantitative (q)PCR analysis are presented in Table SI.

RNA extraction and seq. Total RNA was extracted using TRIzol® (Ambion; Thermo Fisher Scientific, Inc.) and treated with RQ1 RNase-Free DNase (Promega Corporation) to remove DNA. The integrity of RNA was assessed using 1.5% agarose gel electrophoresis. The mRNA was purified using VAHTS mRNA capture beads (cat. no. N401-01, Vazyme, China) For each sample, 1 μ g of total RNA was used for RNA-seq library preparation. The purified RNA was treated with RQ1 DNase (Promega) to remove DNA before used for directional RNA-seq library preparation by KAPA Stranded mRNA-Seq Kit for Illumina® Platforms (cat. no. KK8544, Roche). Polyadenylated mRNAs were purified and fragmented. Fragmented mRNAs were converted into double strand cDNA. Following end repair and A tailing, the DNAs were ligated to Diluted Roche Adaptor (KK8726, Roche). After purification of ligation product and size fractioning to 300-500 bps, the ligated products were amplified and purified, quantified and stored at -80°C before sequencing. The strand marked with dUTP (the 2nd cDNA strand) is not amplified, allowing strand-specific sequencing.

For high-throughput sequencing, the libraries were prepared following the manufacturer's instructions and applied to Illumina Novaseq 6000 system for 150 nt paired-end sequencing.

RNA-seq raw data cleaning and alignment. Original reads containing more than 2 uncertain bases were discarded. The adapter and low-quality bases were trimmed from the original sequencing reads using Fasxtoolkit (version 0.0.13; hannonlab.cshl.edu/fastx_toolkit/index.html). Subsequently, the cleaned reads were aligned to the GRCh38 genome using TopHat2 (20) which allowed a maximum of four misread errors. A single mapped survey was used for counting genetic surveys and calculating fragments per kilobase of transcript per million fragments mapped (FPKM) values (21).

Differentially expressed genes (DEGs) and alternative splicing (AS) analysis. Principal component analysis (PCA, performed by R package factoextra (<https://cloud.r-project.org/package=factoextra>)). demonstrated a separation between Control and ANRIL overexpression samples The edgeR

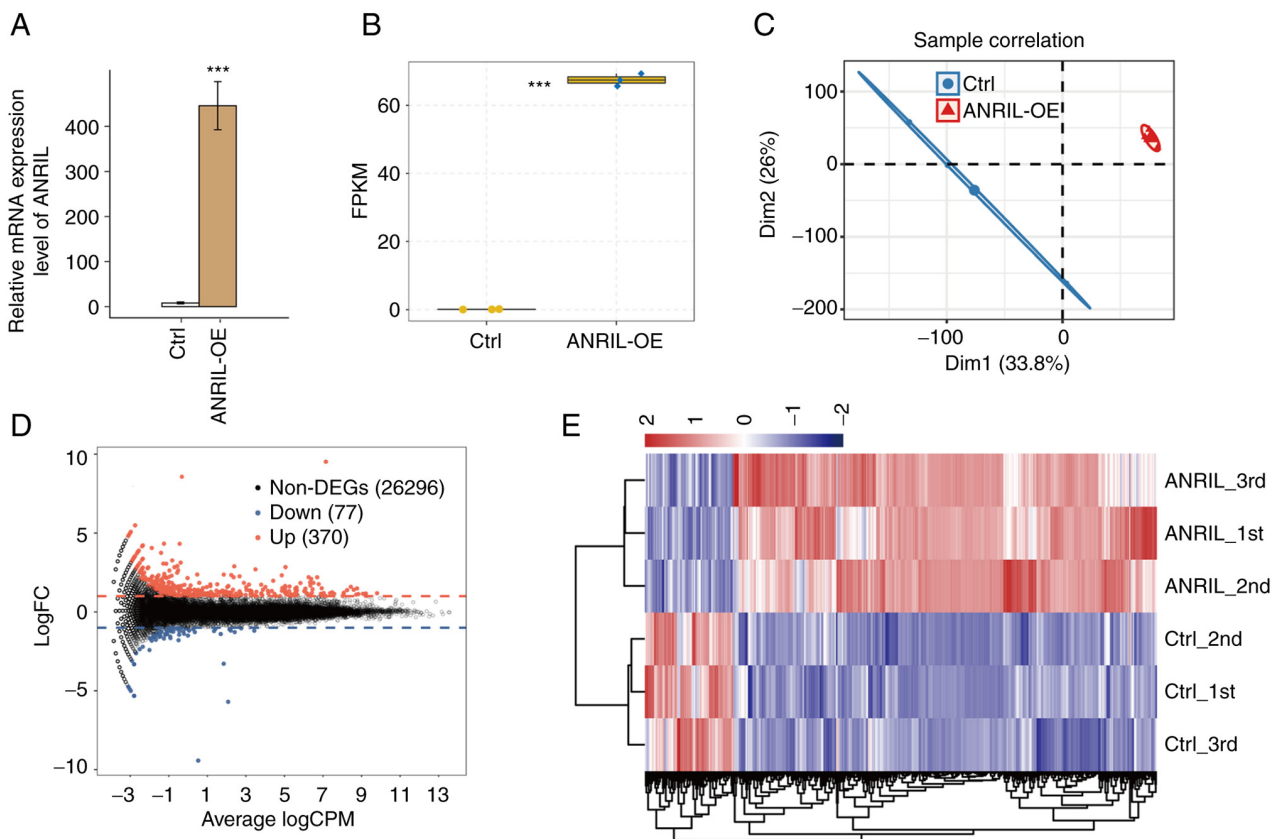


Figure 1. ANRIL overexpression affects gene expression profile of HUVECs. (A) ANRIL mRNA expression levels were quantified using reverse transcription-quantitative PCR. *** $P < 0.001$ vs. Ctrl. (B) Relative ANRIL expression was quantified using RNA-sequencing. (C) Principal component analysis demonstrated a separation between Ctrl and ANRIL overexpression samples. (D) Volcano plot of ANRIL-regulated genes. (E) Hierarchical clustering of DEGs in Ctrl and ANRIL overexpression samples. Fragments per kilobase of transcript per million fragments mapped values were \log_2 -transformed and median-centered by each gene. Upregulated, red; downregulated, blue. HUVECs, human umbilical vein endothelial cells; ANRIL, lncRNA-antisense non-coding RNA in the INK4 locus; Ctrl, control; Dim, dimension; Fold Change(FC), Counts-Per-Million(CPM).

Bioconductor package (version no. 3.32.1) (22) was used to assess DEGs. The fold-change (FC) of the DEGs, \log_2FC and false discovery rate (FDR) were obtained following testing. The cutoff thresholds were set to a FC of ≥ 2 or ≤ -2 and FDR < 0.05 . To clean up the feature categories in DEGs, the KOBAS 2.0 server was used to determine the Gene Ontology (GO) terminology and Kyoto Encyclopedia of Genes and Genomes (KEGG) path (23).

AS events (ASEs) and regulated ASEs (RASEs) between the samples were defined and quantified using the ABLas pipeline (24,25). Briefly, the ABLas pipeline was used to assess ten types of ASE based on the splice junction reads, including exon skipping (ES), mutually exclusive exons (MXE), alternative 5' splice site (A5SS), intron retention (IR), alternative 3' splice site (A3SS), mutually exclusive 3' UTRs (3pMXE), mutually exclusive 5' UTRs (5pMXE), cassette exon, A3SS + ES and A5SS + ES. To evaluate the validity of the RNA-seq data, RT-qPCR was performed as aforementioned for selected DEGs ((CEBPB, CXCL11, PTGS2, THEMIS2, IL6, HMOX1, NLRC5, SECTM1, TNFSF18 and TRIM21) and ASEs (CTNNB1, IL23, ATP13A2, SIGIRR, HDAC7, and normalized using the reference gene GAPDH. The same RNA samples for RNA-seq were used for RT-qPCR and are available from the Gene Expression Omnibus website using accession number GSE197115 (ncbi.nlm.nih.gov/geo/query/acc.cgi?acc=GSE197115).

Statistical analysis. An unpaired two-tailed t-test (between two groups) was performed for cell and RT-qPCR data. $P < 0.05$ was considered to indicate a statistically significant difference. The data are presented as the mean \pm standard deviation. GraphPad Prism (version no. 8.0; GraphPad Software, Inc.) was used to perform unpaired Student's t-test. Each experiment was performed for at least three biological replicates, except RNA-seq.

Results

RNA-seq analysis of ANRIL-regulated transcriptome profile in HUVECs. RNA-seq was used to explore the molecular mechanisms of ANRIL-mediated transcriptional regulation. ANRIL was overexpressed in HUVECs following transfection using a vector expressing ANRIL (ANRIL-OE) compared with empty negative control vector (NC). The results of RT-qPCR demonstrated that ANRIL mRNA expression levels were significantly increased in HUVECs with ANRIL-OE (Fig. 1A and B). A total of six RNA-seq libraries were constructed and sequenced for the ANRIL-OE and NC group with each group having three biological repeats (ANRIL_1st, ANRIL_2nd, ANRIL_3rd, Ctrl_1st, Ctrl_2nd and Ctrl_3rd). For high-throughput sequencing, the library was prepared according to the manufacturer's protocols and used the Illumina NovaSeq 6000 system for terminal sequencing to

Table I. Summary of RNA-seq reads used in analysis.

Sample	ANRIL_1st	ANRIL_2nd	ANRIL_3rd	Ctrl_1st	Ctrl_2nd	Ctrl_3rd	Mean ± SD
Raw	71189488	68752622	82908788	71254178	81115056	69881880	74183668±6159878
Clean (%)	69634309 (97.82)	67136142 (97.65)	81023158 (97.73)	69873252 (98.06)	79428266 (97.92)	68291552 (97.72)	72564447±6036790
Total mapped ^a (%)	66924893 (97.62)	64433515 (97.6)	77763393 (97.6)	67444711 (97.92)	76559923 (97.89)	65803658 (97.88)	69821682±5791250
Total uniquely mapped ^b (%)	61071119 (91.25)	58348374 (90.56)	67865079 (87.27)	62954592 (93.34)	70991974 (92.73)	59635640 (90.63)	63477796±4956815
Splice reads ^c (%)	24821085 (40.64)	24093961 (41.29)	27782615 (40.94)	25306098 (40.2)	29117397 (41.02)	25457522 (42.69)	26096446±1930734

^aPaired-end reads that were mapped to the genome; ^bunique reads mapped out of the total mapped reads; ^cuniquely mapped reads that were mapped to splice site. ANRIL, lncRNA-antisense non-coding RNA in the INK4 locus; Ctrl, control.

produce 150 nucleotide paired-end reads. A mean total of 74.18±6.15 million original reads were produced for each sample. After the adapter and polluted sequences were removed, each sample had a mean total of 72.56±6.03 million clean reads. The average number of read pairs/sample was 69.82±2.79 million, which were aligned with the human genome (Table I).

FPKM values were calculated to represent levels of gene expression. RNA-seq yielded robust expression results for 60,498 genes (Table II). A correlation matrix was calculated based on the FPKM value of the expression gene in all samples. There was a high Pearson's correlation value between ANRIL-OE and the control (>0.99), which indicated similar expression of most genes. Furthermore, significant segregation between the sample groups was demonstrated in the FPKM uniform numerical sequence for DEGs, indicating agreement between the composite datasets (Fig. 1C and E). These results indicated that expression of lncRNA-ANRIL altered the replication level of genes. To further compare the gene expression profile, edgeR was performed to identify the DEGs between the ANRIL-OE and control cells, with a cut-of as fold change ≥2 or ≤0.5 and a 5% false discovery rate (FDR) (22). A total of 370 up- and 77 downregulated genes were identified between ANRIL-OE and NC cells. Indicating that ANRIL overexpression extensively regulates gene expression in HUVECs (Fig. 1D).

ANRIL regulates expression of genes involved in the inflammatory response and IκB/NF-κB signaling pathway in HUVECs. To reveal the potential roles of DEGs, GO functional analysis was performed and 26,743 DEGs were annotated. The results revealed 370 upregulated and 77 downregulated genes annotated with GO categories biological process terms, respectively (Fig. 2A and B; Tables SII and SIII). Upregulated genes were significantly enriched in inflammatory response and NF-κB signaling pathway, including Mullerian-inhibiting factor (AMH), Cystathionine gammalyase (CTH), Heme oxygenase 1 (HMOX1), Kruppel-like factor 4 (KLF4), Protein NLRC5, Secreted and transmembrane protein 1 (SECTM1), Tumor necrosis factor ligand superfamily member 18 (TNFSF18), E3 ubiquitin-protein ligase Tripartite-motif protein 21 (TRIM21),

Table II. Mapped normalized reads on expressed genes in reference genome (60,498 total genes in genome).

Sample	Expressed genes with FPKM >0 (%)	Expressed genes with FPKM ≥1 (%)
ANRIL_1st	21066 (34.82)	11245 (53.38)
ANRIL_2nd	20920 (34.58)	11238 (53.72)
ANRIL_3rd	21319 (35.24)	11254 (52.79)
Ctrl_1st	20980 (34.68)	11392 (54.30)
Ctrl_2nd	20943 (34.62)	11264 (53.78)
Ctrl_3rd	20696 (34.21)	11101 (53.64)

FPKM, fragments per kilobase of transcript per million fragments mapped; Ctrl, control.

CCAAT/enhancer-binding protein beta (CEBPB), C-X-C motif chemokine 10 (CXCL10), C-X-C motif chemokine 11 (CXCL11), IL-1 alpha (IL1A), Interleukin-6 (IL6), Prostaglandin G/H synthase 2 (PTGS2), Protein THEMIS2, Toll-like receptor 3 (TLR3), Tumor necrosis factor alpha-induced protein 3 (TNFAIP3); Fig. 2C and D). These results indicated a key role of ANRIL in expression of inflammatory factors.

To verify the effect of ANRIL-OE on the expression of these DEGs, qPCR was conducted to quantify the changes in mRNA levels of these genes. Ten upregulated DEGs were randomly selected for qPCR analysis, including CEBPB, CXCL11, PTGS2, THEMIS2, IL6, HMOX1, NLRC5, SECTM1, TNFSF18 and TRIM21. These results demonstrated that mRNA expression levels of all 10 selected DEGs were significantly increased, except IL6, which was consistent with RNA sequence analysis (Fig. 2E and F).

When the corrected P-value for the KEGG pathways was set at P<0.05, numerous cancer-associated pathways including 'cytokine-cytokine receptor interaction', 'NF-κB signaling pathway', 'Toll-like receptor signaling pathway', 'TNF signaling pathway' and 'inflammatory mediator regulation of TRP channels' were demonstrated to be enriched (Figs. S1 and S2; Tables SIV and SV).

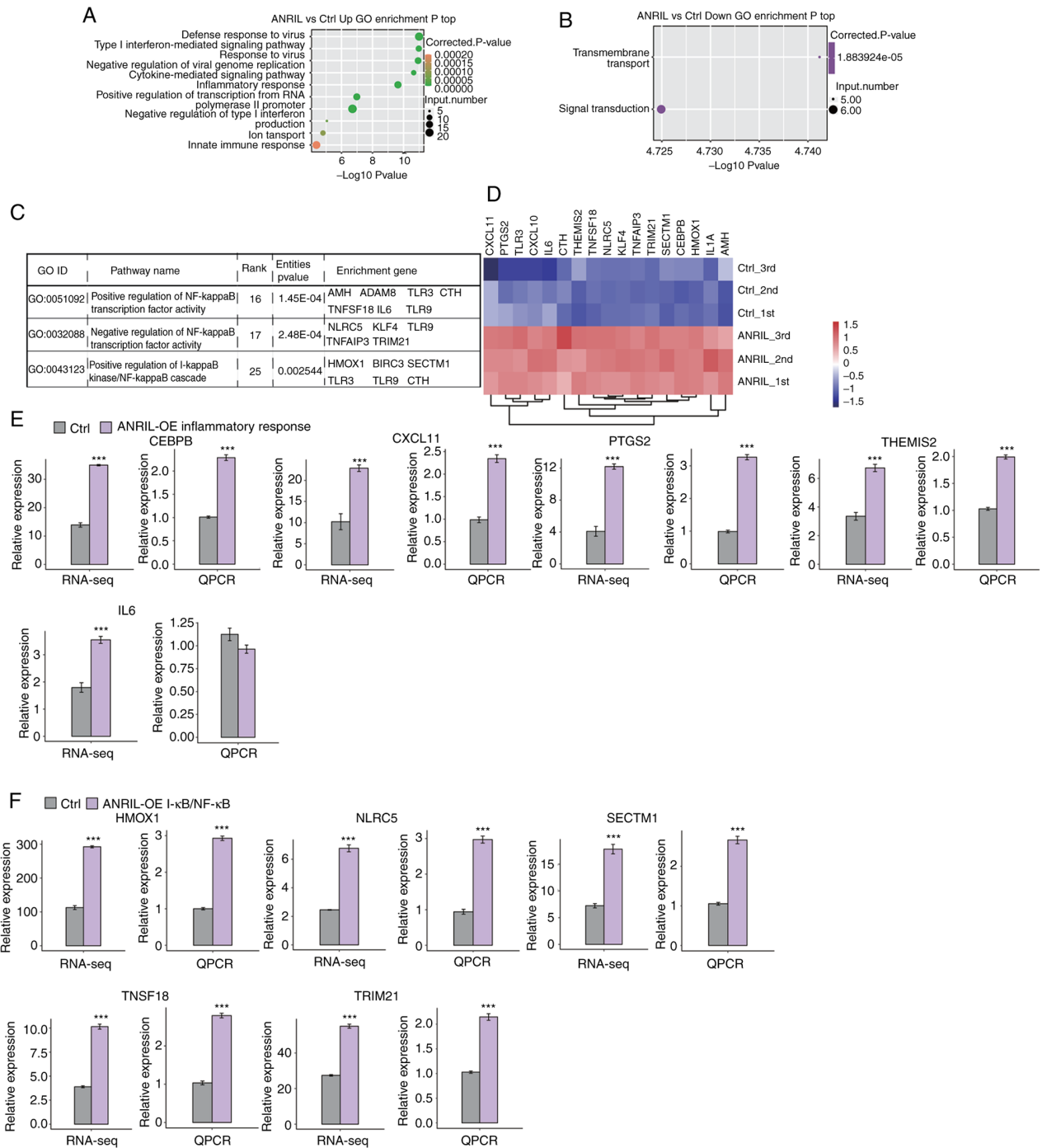


Figure 2. Functional analysis of ANRIL-regulated DEGs in HUVECs. (A) Top 10 GO biological processes of upregulated genes. (B) Top GO biological processes of downregulated genes. (C) ANRIL-upregulated genes were enriched in NF- κ B-associated pathways. (D) Hierarchical clustering of the expression levels of inflammatory response and NF- κ B-associated genes effected by ANRIL overexpression in HUVECs. (E) Gene expression levels of ANRIL-regulated inflammatory response genes assessed using RNA-seq data. (F) Relative expression levels of DEGs identified using RNA-seq were assessed using RT-qPCR. For RT-qPCR, GAPDH was used as the reference gene. Student's t test was performed to compare ANRIL-OE and control cells. **** $P < 0.001$ vs. Ctrl. HUVECs, human umbilical vein endothelial cells; ANRIL, lncRNA-antisense non-coding RNA in the INK4 locus; DEGs, differentially expressed genes; GO, Gene Ontology; Ctrl, control; CEBPB, CCAAT/enhancer binding protein (C/EBP) beta; CXCL11, chemokine (C-X-C motif) ligand 11; PTGS2, prostaglandin-endoperoxide synthase 2; THEMIS2, thymocyte selection associated family member 2; IL6, interleukin 6; HMOX1, heme oxygenase 1; TRIM21, tripartite motif containing 21; SECTM1, secreted and transmembrane 1; TNFSF18, tumor necrosis factor (ligand) superfamily, member 18; NLRCS, Protein NLRCS.

ANRIL overexpression regulates AS of transcription factors in HUVECs. To the best of our knowledge, there have been few previous reports of studies of regulation of AS of ANRIL in HUVECs. The purpose of the present study was to elucidate the role of ANRIL in the regulation of AS. It was hypothesized that by regulating the expression of key functional genes,

ANRIL may be involved in regulating inflammatory responses. Therefore, whether ANRIL affected expression of DEGs via AS regulation was evaluated. The splice reads from ANRIL-OE and NC HUVECs were mapped to the reference genome and 203,974 exons annotated (55.53% of total annotated ones). Next, a total of 134,447 known splice sites and 51,606 novel

Table III. Known or novel splicing events detected using the ABLas pipeline.

A, Known splicing events												
Sample	3pMXE	5pMXE	A3SS	A3SS + ES	A5SS	A5SS + ES	ES	IR	MXE	Cassette exon	Total	Detected junctions
ANRIL_1st	963	1443	6030	673	6045	763	3268	4514	357	1787	25843	179431
ANRIL_2nd	980	1529	5915	640	6113	768	3288	4441	378	1775	25827	178905
ANRIL_3rd	999	1632	6288	681	6357	801	3380	4696	386	1896	27116	186053
Ctrl_1st	922	1489	5799	582	6078	735	3126	4439	343	1756	25269	178976
Ctrl_2nd	940	1555	5916	594	6142	800	3176	4388	373	1845	25729	180273
Ctrl_3rd	918	1453	5600	591	5780	738	3036	4186	317	1701	24320	173350
Total	2390	3959	14507	1699	14629	1856	6596	8584	842	3481	58543	300041
B, Novel splicing events												
Sample	3pMXE	5pMXE	A3SS	A3SS&ES	A5SS	A5SS&ES	ES	IR	MXE	Cassette exon	Total	Detected junctions
ANRIL_1st	657	1005	3468	401	3258	383	1320	3249	131	477	14349	47618
ANRIL_2nd	672	1032	3404	371	3235	387	1320	3173	134	459	14187	46874
ANRIL_3rd	688	1149	3641	391	3415	428	1352	3391	143	505	15103	51606
Ctrl_1st	614	1010	3145	304	3160	359	1142	3135	126	409	13404	42558
Ctrl_2nd	628	1036	3290	306	3136	407	1135	3083	136	422	13579	44500
Ctrl_3rd	628	966	3095	310	2962	380	1100	2934	104	366	12845	40754
Total	1912	3185	10649	1267	10156	1284	3652	6951	424	1400	40880	140131

3pMXE, mutually exclusive 3' UTRs; 5pMXE, mutually exclusive 5' UTRs; A3SS, alternative 3' splice site; ES, exon skipping; A5SS, alternative 5' splice site; IR, intron retention; MXE, mutually exclusive exons.

splice junctions were identified using TopHat2. AS events in the spliced joints were identified using the ABLas pipeline (25,16), which resulted in 58,543 known alternative splicing events (ASEs) and 40,880 novel ASEs (Tables II and III).

A strict cut-off value $P \leq 0.05$ and modified T-value ≥ 0 were used to identify RASEs with high confidence adjustment. A total of 1,714 RASEs was identified. ASEs regulated by ANRIL included 330 ES, 296 A5SS, 286 A3SS and 191 cassette exons (Fig. 3A). To analyze whether the increase in ASEs was due to altered transcription, we overlapped the genes whose level of expression and alternative splicing were both regulated by ANRIL, and identified twenty one such genes: LINC01002, NPIP4, TXNRD1, OAS1, SLC3A2, NBP14, STX1A, LINC01063, DDX60L, CTB-5506.8, RP11-875011.1, DDIT3, FXD2, MEF2B, MX1, WARS, IFITM1, NBP26, PI4KAP1, SLC22A20 and PSAT1 (Fig. 3B). These results suggested that transcriptional regulation and AS may be linked.

GO analysis was performed to assess the potential features of regulated AS genes (RASGs). The results demonstrated that RASGs were enriched in GO biological processes, such as 'gene expression', 'translation', 'DNA repair', 'RNA processing' and 'positive regulation of the I κ B kinase/NF- κ B signaling pathway' (Fig. 3C). Enriched KEGG pathways ($P < 0.05$) included 'RNA transport', 'Notch signaling pathway', 'axon guidance', 'apoptosis' and 'VEGF signaling pathway' (Fig. 3D). These results demonstrated that ANRIL overexpression affected expression of DEGs and including inflammatory response by regulating AS of transcription factors and co-activators. To evaluate ASEs identified using the RNA-Seq data, five possible ASEs were assessed using RT-qPCR. The five events validated by RT-qPCR were consistent with RNA-Seq results. The five genes which contained verified splicing events were as follows: Catenin Beta 1 (CTNNB1), IL23, ATPase type 13A2 (ATP13A2), Single Immunoglobulin and Toll-interleukin 1 Receptor domain (SIGIRR) and Histone Deacetylase 7A (HDAC7) (Fig. 3E and F; Fig. S3A-C).

Discussion

In the immune system, lncRNAs serve a key role in regulating cell survival, inflammation and angiogenesis (4,9,10). The effect of ANRIL on the occurrence of IS has been previously reported by numerous studies (9,10). However, the specific mechanism remains unknown. The inflammatory response may be an important regulatory pathway. Here, ANRIL overexpression regulated the expression of genes associated with inflammatory responses, activated the NF- κ B signaling pathway and affected the AS of certain genes (CTNNB1, IL23) with key functions in the inflammatory response in HUVECs.

In the occurrence and development of IS, inflammation serves a key role. Numerous studies (26,27) have reported that ANRIL promotes the inflammatory response, leading to angiogenesis and vascular endothelial injury, which is similar to the results of GO analysis following high-throughput sequencing in the present study. But these results were inconsistent with respect to the inflammatory reaction and mRNA expression levels of ANRIL in cells and tissue, which suggested that ANRIL acted as an anti-inflammatory gene participating in acute IS progression (28,29). This evidence

indicated that ANRIL may serve a bidirectional role in the pathological process of IS, which can alleviate nerve injury by activating vascular endothelial growth factors and promote inflammatory progress of IS via the NF- κ B signaling pathway. It has been reported that a number of lncRNAs are abnormally expressed in inflammatory disease and participate in activating numerous inflammation-associated genes and signaling pathways (30). It has also been indicated that lncRNA changes in IS are present and provide a unique view of multiple adjustment genes in ANRIL-OE cells, which are significantly enriched in inflammatory reactions and the NF- κ B pathway. Certain of these gene (NLRC5, CEBPB, PTGS2) had not been reported to be associated with ANRIL regulation in previous studies. Among these genes, lncRNAs promotes inflammation by regulating genes such as lncRNA MALAT1, which regulates PTGS2 by targeting microRNA-26b to aggravated inflammatory reactions in myocardial ischemia-reperfusion injury (31). Moreover, Liu *et al* (32) reported that downregulation of NLRC5 decreases cell apoptosis and intracellular oxidative stress in an acute myocardial infarction model rat, which was regulated by lncRNA. Certain studies have also reported that CEBPB and IL6 genes were regulated by lncRNAs and involved in the inflammatory response (33,34). Furthermore, Liu *et al* (35) reported that ANRIL regulates HUVEC dysfunction by regulating the let-7b/TGF- β R1 signaling pathway to mediate the development of atherosclerosis. Knockdown of ANRIL significantly promoted cell proliferation and tubule formation and inhibited inflammatory activation and apoptosis of HUVEC. Other previous studies reported that lncRNA-ANRIL knockdown inhibits proliferation and migration of oxidized low-density lipoprotein-induced HUVECs by sponging microRNA-339-5p and inactivating the RAS/RAF/ERK signaling pathway (36,37). To the best of our knowledge, however, there is a lack of research on the regulation of other genes by lncRNAs. The results of present study suggested that lncRNA-ANRIL regulated these genes (NLRC5, CEBPB) to participate in the inflammatory response. These findings extend understanding of the role of ANRIL in the inflammatory response. Furthermore, the identification of downstream genes provides additional possible research directions.

NF- κ B, a classical nuclear transcription factor, has been reported to be involved in inflammation and cell survival (4). Many of the upregulated genes in ANRIL-OE cells were enriched in 'NF- κ B pathway'. These genes may affect the NF- κ B signaling pathway as downstream regulatory genes of ANRIL. The study on the correlation between upregulated genes and lncRNAs have reported that lncRNAs regulate the NF- κ B signaling pathway via certain genes, such as caspase recruitment domain family member 8 (CARD8) which is the target of ANRIL and that ANRIL is an inhibitor of the NF- κ B signaling pathway (38). Activation of ANRIL inhibits the inflammatory process by inhibiting NF- κ B signaling pathway via activation of CARD8. The present study identified potential controlled by lncRNA ANRIL that regulate the NF- κ B signaling pathway. Certain genes have been confirmed to exist in the lncRNA/NF- κ B regulatory pathway, including KLF4 and NLRC5. KLF4 decrease transcription activity of NF- κ B by establishing a positive feedback loop of NF- κ B/KLF4, which is controlled by NF- κ B-interacting lncRNA (39), and

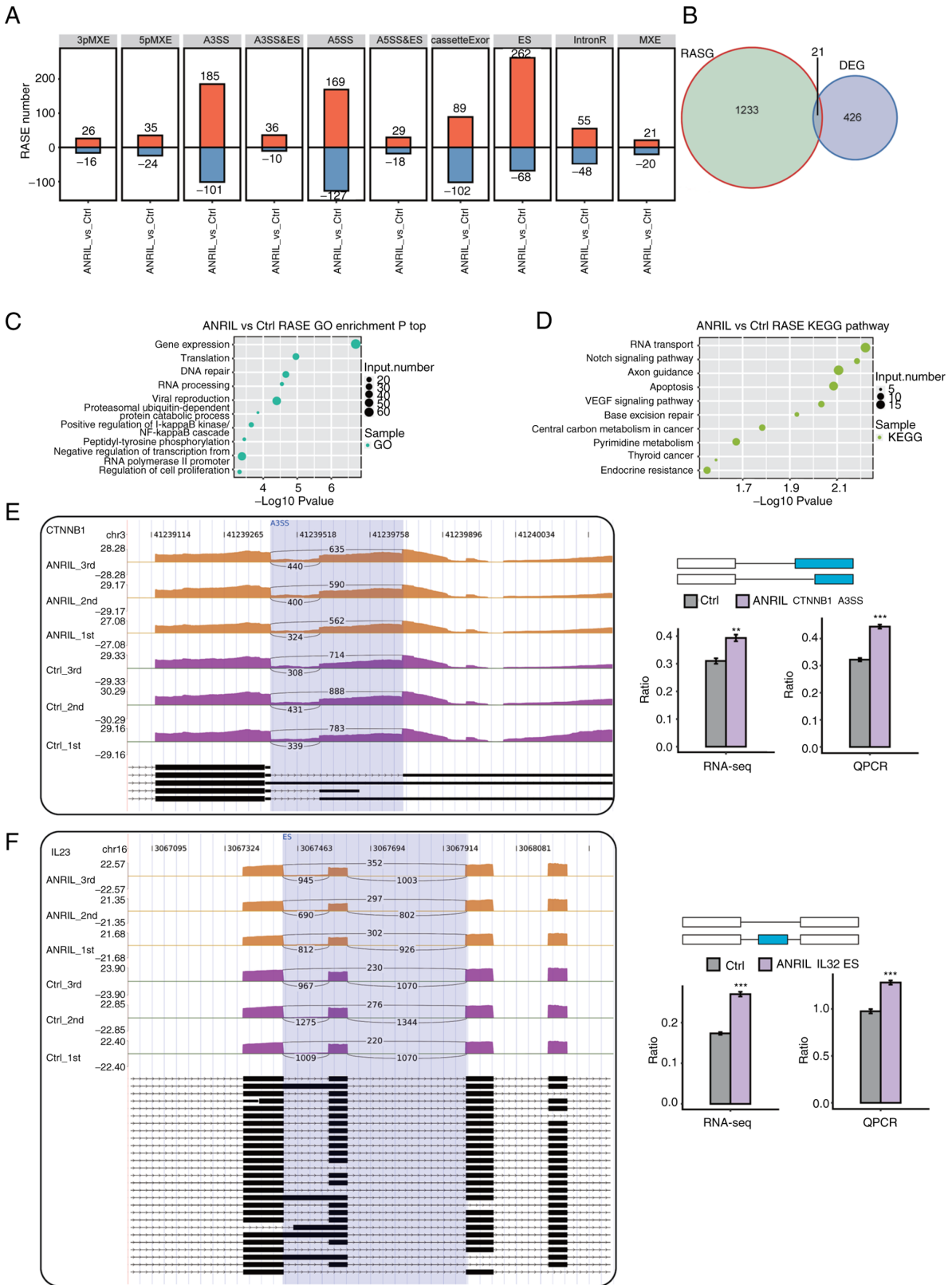


Figure 3. AS pattern analysis following ANRIL overexpression in HUVECs. (A) Frequency distribution of types of ANRIL-regulated ASEs. (B) Overlap analysis between DEGs and ANRIL-RASGs. Top 10 (C) GO biological processes and (D) KEGG pathways identified for RASGs. Integrative Genomics Viewer-sashimi plots of ANRIL-regulated (E) A3SS of CTNNB1 and (F) ES of IL32 demonstrate AS changes in ANRIL overexpression and control cells; transcripts for the gene presented below. The schematic diagrams depicts the structures of ASEs, The exon sequences were denoted by boxes and intron sequences by horizontal lines. RNA-seq quantification and RT-qPCR validation of ASEs were presented in the histogram. The altered ratio of AS events in RNA-seq data was calculated as follows: AS1 junction reads/(AS1 junction reads + AS2 junction reads). The altered ratio of AS events in RT-qPCR data was calculated as follows: AS1 transcript level/AS2 transcript level. Student's t test was performed to compare ANRIL-OE and Ctrl cells. **P<0.01 and ***P<0.001 vs. Ctrl. DEGs, differentially expressed genes; RASGs, regulated alternative splicing genes; HUVECs, human umbilical vein endothelial cells; ANRIL, lncRNA-antisense non-coding RNA in the INK4 locus; GO, Gene Ontology; KEGG, Kyoto Encyclopedia of Genes and Genomes; A3SS, alternative 3' splice site; ES, exon skipping; ASEs, alternative splicing events; RNA-seq, RNA-sequencing; RT-qPCR, reverse transcription-quantitative PCR; Ctrl, control.

lncRNA ARID 2-IR, which was located within the intron region between the fourth and fifth exons of Arid2 on the chromosome 15 of the mouse genome, mediates renal inflammation driven by NF- κ B via a NLRC5-dependent mechanism (40). To the best of our knowledge, however, the role of genes in the ANRIL/NF- κ B regulatory pathway remains unknown. GO and KEGG analysis in the present study demonstrated the identity of candidate genes, which need to be assessed by further tests.

AS is a process in which exons are included or excluded from the final mRNA transcripts, thus allowing genes to produce several isoforms with cell- and tissue-specific functions. AS and its role in transcript diversity is critical to the susceptibility and severity of disease and different types of AS have previously been reported following stroke (41). In previous study, only a few lncRNAs were reported to have an important role in RNA splicing (42). In the present study, ANRIL was a multifunctional lncRNA that regulated both AS and translation and ASEs occurred in genes involved in the inflammatory response, including CTNNB1, IL32, ATP13A2, SIGIRR and HDAC7. SIGIRR, a negative regulator of the TLR signaling pathway, has been reported to attenuate colonic tissue inflammation via inhibition of TLR4/NF- κ B overactivation by downregulating TLR4, MyD88 and NF- κ B p65 expression in a mouse model of colitis (43). HDACs drive innate immune cell-mediated inflammation and serve as key molecular links between TLR-inducible aerobic glycolysis and macrophage inflammatory responses (44). CTNNB1, which is a central mediator in the canonical Wnt signaling pathway, has been extensively reported to serve an oncogenic role in numerous types of cancer and stimulate proliferation of microvascular endothelial cells (45,46). Moreover, it has been reported that lncRNAs facilitate tumor progression by targeting CTNNB1 to activate the Wnt/ β -catenin signaling pathway (47,48). The present study identified CTNNB1 as an ANRIL-regulated AS gene, which indicated that CTNNB1-dependent transcriptional regulation may be involved in the inflammatory response. The findings of the present study regarding AS of multiple genes mediated by ANRIL suggested a more complex network between these inflammatory response genes.

The present study had certain limitations. First, it focused on the effects of lncRNA ANRIL on inflammatory-associated pathways in HUVECs but further studies are required to elucidate the underlying molecular mechanism of the effects in HUVECs and other types of cell in detail. Second, there was a lack of research on protein expression levels and additional experiments are needed to demonstrate the effect on protein expression levels. Furthermore, future studies using animal models and patient tissue samples should be conducted to elucidate the mechanism underlying ANRIL-mediated effects *in vivo*.

In the present study, it was demonstrated that ANRIL was involved in the inflammatory response and genetic transcription of NF- κ B. These findings may provide a new direction for the understanding of vascular disease and tumorigenesis, which need to be further evaluated by future studies.

Acknowledgements

The authors would like to thank Dr Weili Quan and Mr Ning Li (both Center for Genome Analysis, ABLife Inc., Wuhan, Hubei, China) for helpful discussions.

Funding

No funding was received.

Availability of data and materials

All data generated or analyzed during the present study are available from the corresponding author on reasonable request.

Authors' contributions

AW and JM conceived and designed the experiments. AW, XL, LD, JL, MS and DFH performed the experiments and constructed the table and figures. XL, LD, MS and JL provided the reagents, materials and analysis tools. AW and JM wrote the paper. JL, DFH, MS and JM revised the manuscript. All authors read and approved the final version of the manuscript. AW, XL, LD, JL, MS, DH and JM confirm the authenticity of all the raw data.

Ethics approval and consent to participate

Not applicable.

Patient consent for publication

Not applicable.

Competing interests

The authors declare that they have no competing interests.

References

- Ren W and Yang X: Pathophysiology of long non-coding RNAs in ischemic stroke. *Front Mol Neurosci* 11: 96, 2018.
- Grammatikakis I and Lal A: Significance of lncRNA abundance to function. *Mamm Genome* 33: 271-280, 2021.
- Lorenzen JM and Thum T: Long noncoding RNAs in kidney and cardiovascular diseases. *Nat Rev Nephrol* 12: 360-373, 2016.
- Statello L, Guo CJ, Chen LL and Huarte M: Gene regulation by long non-coding RNAs and its biological functions. *Nat Rev Mol Cell Biol* 22: 96-118, 2021.
- Chen S, Wu Y, Qin X, Wen P, Liu J and Yang M: Global gene expression analysis using RNA-seq reveals the new roles of panax notoginseng saponins in ischemic cardiomyocytes. *J Ethnopharmacol* 268: 113639, 2021.
- Bao MH, Szeto V, Yang BB, Zhu SZ, Sun HS and Feng ZP: Long non-coding RNAs in ischemic stroke. *Cell Death Dis* 9: 281, 2018.
- Folkersen L, Kyriakou T, Goel A, Peden J, Mälarstig A, Paulsson-Berne G, Hamsten A, Watkins H, Franco-Cereceda A, Gabrielsen A, *et al*: Relationship between CAD risk genotype in the chromosome 9p21 locus and gene expression. Identification of eight new ANRIL splice variants. *PLoS One* 4: e7677, 2009.
- Chen W, Bharati S, Yi L, Benowitz L, Chen Q, Zhang Z, Patel NJ, Aziz-Sultan AM, Chiocca AE and Wang X: Monogenic, polygenic, and microRNA markers for ischemic stroke. *Mol Neurobiol* 56: 1330-1343, 2019.
- Amouyel P: From genes to stroke subtypes. *Lancet Neurol* 11: 931-933, 2012.
- Bai N, Liu W, Xiang T, Zhou Q, Pu J, Zhao J, Luo D, Liu X and Liu H: Genetic association of ANRIL with susceptibility to Ischemic stroke: A comprehensive meta-analysis. *PLoS One* 17: e0263459, 2022.
- Sun R, Wang L, Guan C, Cao W and Tian B: Carotid atherosclerotic plaque features in patients with acute ischemic stroke. *World Neurosurg* 112: e223-e228, 2018.

12. Zhang L, Luo X, Chen F, Yuan W, Xiao X, Zhang X, Dong Y, Zhang Y and Liu Y: LncRNA SNHG1 regulates cerebrovascular pathologies as a competing endogenous RNA through HIF-1 α /VEGF signaling in ischemic stroke. *J Cell Biochem* 119: 5460-5472, 2018.
13. Mo Y, Sun YY and Liu KY: Autophagy and inflammation in ischemic stroke. *Neural Regen Res* 15: 1388-1396, 2020.
14. Zhong W, Li YC, Huang QY and Tang XQ: LncRNA ANRIL ameliorates oxygen and glucose deprivation (OGD) induced injury in neuron cells via miR-199a-5p/CAV-1 axis. *Neurochem Res* 45: 772-782, 2020.
15. Fang X, Hu J and Zhou H: Knock-down of long non-coding RNA ANRIL suppresses mouse mesangial cell proliferation, fibrosis, inflammation via regulating Wnt/ β -Catenin and MEK/ERK pathways in diabetic nephropathy. *Exp Clin Endocrinol Diabetes* 130: 30-36, 2022.
16. Liu B, Cao W and Xue J: LncRNA ANRIL protects against oxygen and glucose deprivation (OGD)-induced injury in PC-12 cells: Potential role in ischaemic stroke. *Artif Cells Nanomed Biotechnol* 47: 1384-1395, 2019.
17. Zhao JH, Wang B, Wang XH, Wang JR and Xu CW: Influence of lncRNA ANRIL on neuronal apoptosis in rats with cerebral infarction by regulating the NF- κ B signaling pathway. *Eur Rev Med Pharmacol Sci* 23: 10092-10100, 2019.
18. Zhang B, Wang D, Ji TF, Shi L and Yu JL: Overexpression of lncRNA ANRIL up-regulates VEGF expression and promotes angiogenesis of diabetes mellitus combined with cerebral infarction by activating NF- κ B signaling pathway in a rat model. *Oncotarget* 8: 17347-17359, 2017.
19. Livak KJ and Schmittgen TD: Analysis of relative gene expression data using real-time quantitative PCR and the 2(-Delta Delta C(T)) method. *Methods* 25: 402-408, 2001.
20. Kim D, Pertea C, Trapnell H, Pimentel R, Kelley R and Salzberg SL: TopHat2: Accurate alignment of transcriptomes in the presence of insertions, deletions and gene fusions. *Genome Biol* 14: R36, 2013.
21. Trapnell CBA, Williams G, Pertea A, Mortazavi G, Kwan MJ, van Baren SL, Salzberg SL, Wold BJ and Pachter L: Transcript assembly and quantification by RNA-Seq reveals unannotated transcripts and isoform switching during cell differentiation. *Nat Biotechnol* 28: 511-515, 2010.
22. Robinson MD, McCarthy DJ and Smyth GK: edgeR: A Bioconductor package for differential expression analysis of digital gene expression data. *Bioinformatics* 26: 139-140, 2010.
23. Xie CX, Mao J, Huang Y, Ding J, Wu S, Dong L, Kong G, Gao C, Li CY and Wei L: KOBAS 2.0: A web server for annotation and identification of enriched pathways and diseases. *Nucleic Acids Res* 39(Web Server issue): W316-W322, 2011.
24. Xia H, Chen D, Wu Q, Wu G, Zhou Y, Zhang Y and Zhang L: CELF1 preferentially binds to exon-intron boundary and regulates alternative splicing in HeLa cells. *Biochim Biophys Acta Gene Regul Mech* 1860: 911-921, 2017.
25. Jin L, Li G, Yu D, Huang W, Cheng C, Liao S, Wu Q and Zhang Y: Transcriptome analysis reveals the complexity of alternative splicing regulation in the fungus *Verticillium dahliae*. *BMC Genomics* 18: 130, 2017.
26. Liu HW, Hu ZL, Li H, Tan QF, Tong J and Zhang YQ: Knockdown of lncRNA ANRIL suppresses the production of inflammatory cytokines and mucin 5AC in nasal epithelial cells via the miR-15a-5p/JAK2 axis. *Mol Med Rep* 23: 145, 2021.
27. Zhou B, Li L, Qiu X, Wu J, Xu L and Shao W: Long non-coding RNA ANRIL knockdown suppresses apoptosis and pro-inflammatory cytokines while enhancing neurite outgrowth via binding microRNA-125a in a cellular model of Alzheimer's disease. *Mol Med Rep* 22: 1489-1497, 2020.
28. Feng L, Guo J and Ai F: Circulating long noncoding RNA ANRIL downregulation correlates with increased risk, higher disease severity and elevated pro-inflammatory cytokines in patients with acute ischemic stroke. *J Clin Lab Anal* 33: e22629, 2019.
29. Holdt LM, Stahring A, Sass K, Pichler G, Kulak NA, Wilfert W, Kohlmaier A, Herbst A, Northoff BH, Nicolaou A, *et al*: Circular non-coding RNA ANRIL modulates ribosomal RNA maturation and atherosclerosis in humans. *Nat Commun* 7: 12429, 2016.
30. Zhang X, Tang X, Liu K, Hamblin MH and Yin KJ: Long noncoding RNA Malat1 regulates cerebrovascular pathologies in ischemic stroke. *J Neurosci* 37: 1797-1806, 2017.
31. Ruan Z, Wang S, Yu W and Deng F: LncRNA MALAT1 aggravates inflammation response through regulating PTGS2 by targeting miR-26b in myocardial ischemia-reperfusion injury. *Int J Cardiol* 288: 122, 2019.
32. Liu Z, Liu J, Wei Y, Xu J, Wang Z, Wang P, Sun H, Song Z and Liu Q: LncRNA MALAT1 prevents the protective effects of miR125b5p against acute myocardial infarction through positive regulation of NLRC5. *Exp Ther Med* 19: 990-998, 2020.
33. Wu H, Liu B, Chen Z, Li G and Zhang Z: MSC-induced lncRNA HCP5 drove fatty acid oxidation through miR-3619-5p/AMPK/PGC1 α /CEBPB axis to promote stemness and chemo-resistance of gastric cancer. *Cell Death Dis* 11: 233, 2020.
34. Jiang L and Li J: lncRNA GMDS-AS1 upregulates IL-6, TNF- α and IL-1 β , and induces apoptosis in human monocytic THP-1 cells via miR-96-5p/caspase 2 signaling. *Mol Med Rep* 25: 67, 2022.
35. Liu X, Li S, Yang Y, Sun Y, Yang Q, Gu N, Li J, Huang T, Liu Y, Dong H, *et al*: The lncRNA ANRIL regulates endothelial dysfunction by targeting the let/TGF- β R1 signalling pathway. *J Cell Physiol* 236: 2058-2069, 2020.
36. Huang T, Zhao HY, Zhang XB, Gao XL, Peng WP, Zhou Y, Zhao WH and Yang HF: LncRNA ANRIL regulates cell proliferation and migration via sponging miR-339-5p and regulating FRS2 expression in atherosclerosis. *J Eur Rev Med Pharmacol Sci* 24: 1956-1969, 2020.
37. Ying Liu X, Li S, Yang Y, Sun Y, Yang Q, Gu N, Li J, Huang T, Liu Y, Dong H, *et al*: The lncRNA ANRIL regulates endothelial dysfunction by targeting the let-7b/TGF- β R1 signalling pathway. *J Cell Physiol* 236: 2058-2069, 2021.
38. Bai Y, Nie S, Jiang G, Zhou Y, Zhou M, Zhao Y, Li S, Wang F, Lv Q, Huang Y, *et al*: Regulation of CARD8 expression by ANRIL and association of CARD8 single nucleotide polymorphism rs2043211 (p.C10X) with ischemic stroke. *Stroke* 45: 383-388, 2014.
39. Zhu X, Du J, Yu J, Guo R, Feng Y, Qiao L, Xu Z, Yang F, Zhong G, Liu F, *et al*: LncRNA NKILA regulates endothelium inflammation by controlling a NF- κ B/KLF4 positive feedback loop. *J Mol Cell Cardiol* 126: 60-69, 2019.
40. Zhang P, Yu C, Yu J, Li Z, Lan HY and Zhou Q: Arid2-IR promotes NF- κ B-mediated renal inflammation by targeting NLRC5 transcription. *Cell Mol Life Sci* 78: 2387-2404, 2020.
41. Suñé-Pou M, Prieto-Sánchez S, Boyero-Corral S, Moreno-Castro C, El Yousfi Y, Suñé-Negre JM, Hernández-Munain C and Suñé C: Targeting splicing in the treatment of human disease. *Genes (Basel)* 8: 87, 2017.
42. Huang JG, Sachdeva M, Xu E, Robinson TJ, Luo L, Ma Y, Williams NT, Lopez O, Cervia LD, Yuan F, *et al*: The long noncoding RNA NEAT1 promotes renal sarcoma metastasis by regulating RNA splicing pathways. *Mol Cancer Res* 18: 1534-1544, 2020.
43. Liu J, Chen Y, Liu D, Liu W, Hu S, Zhou N and Xie Y: Ectopic expression of SIGIRR in the colon ameliorates colitis in mice by downregulating TLR4/NF- κ B overactivation. *Immunol Lett* 183: 52-61, 2017.
44. Gupta KD, Shakespear MR, Curson JEB, Murthy AMV, Iyer A, Hodson MP, Ramnath D, Tillu VA, von Pein JB, Reid RC, *et al*: Class IIa histone deacetylases drive toll-like receptor-inducible glycolysis and macrophage inflammatory responses via pyruvate kinase M2. *Cell Rep* 30: 2712-2728, 2020.
45. Nelson WJ and Nusse R: Convergence of Wnt, beta-catenin, and cadherin pathways. *Science* 303: 1483-1487, 2004.
46. Moon-Sung L, Hee-Jung B, Lee J, Jeoung DI, Kim YM and Lee H: Tetraspanin CD82 represses Sp1-mediated Snail expression and the resultant E-cadherin expression interrupts nuclear signaling of β -catenin by increasing its membrane localization. *J Cell Signal* 52: 83-94, 2018.
47. Chai W, Liu R, Li F, Zhang Z and Lei B: Long noncoding RNA TSLNC8 enhances pancreatic cancer aggressiveness by regulating CTNNB1 expression via association with HuR. *Hum Cell* 34: 165-176, 2021.
48. Pan Z, Ding J, Yang Z, Li H, Ding H and Chen Q: LncRNA FLVCR1-AS1 promotes proliferation, migration and activates Wnt/ β -catenin pathway through miR-381-3p/CTNNB1 axis in breast cancer. *Cancer Cell Int* 20: 214, 2020.

